Cholera toxin inhibits IL-12 production and CD8α+ dendritic cell differentiation by cAMP-mediated inhibition of IRF8 function

Andrea la Sala,[1] Jianping He,[2] Leopoldo Laricchia-Robbio,[4] Stefania Gorini,[1] Akiko Iwasaki,[5] Michael Braun,[6] George S. Yap,[7] Alan Sher,[3] Keiko Ozato,[4] and Brian Kelsall[2]

[1]Laboratory of Molecular and Cellular Immunology, Istituto di Ricovero e Cura a Carattere Scientifico San Raffaele, 00163 Rome, Italy
[2]Mucosal Immunobiology Section, Laboratory of Molecular Immunology, [3]Immunobiology Section, Laboratory of Parasitic Diseases, National Institute of Allergy and Infectious Disease, [4]Laboratory of Molecular Growth Regulation, National Institute of Child Health and Human Development, National Institutes of Health, Bethesda, MD 20892
[5]Department of Immunobiology, Yale University School of Medicine, New Haven, CT 06520
[6]Department of Pediatrics, Division of Pediatric Nephrology and Hypertension, University of Texas Health Science Center–Houston, Houston, TX 77030
[7]Center for Immunity and Inflammation, University of Medicine and Dentistry of New Jersey Medical School, Newark, NJ 07101

Prior studies have demonstrated that cholera toxin (CT) and other cAMP-inducing factors inhibit interleukin (IL)-12 production from monocytes and dendritic cells (DCs). We show that CT inhibits Th1 responses in vivo in mice infected with *Toxoplasma gondii*. This correlated with low serum IL-12 levels and a selective reduction in the numbers of CD8α+ conventional DCs (cDCs) in lymphoid organs. CT inhibited the function of interferon (IFN) regulatory factor (IRF) 8, a transcription factor known to positively regulate IL-12p35 and p40 gene expression, and the differentiation of CD8α+ and plasmacytoid DCs (pDCs). Fluorescence recovery after photobleaching analysis showed that exposure to CT, forskolin, or dibutyryl (db) cAMP blocked LPS and IFN-γ–induced IRF8 binding to chromatin. Moreover, CT and dbcAMP inhibited the binding of IRF8 to the IFN-stimulated response element (ISRE)–like element in the mouse IL-12p40 promoter, likely by blocking the formation of ISRE-binding IRF1–IRF8 heterocomplexes. Furthermore, CT inhibited the differentiation of pDCs from fms-like tyrosine kinase 3 ligand–treated bone marrow cells in vitro. Therefore, because IRF8 is essential for IL-12 production and the differentiation of CD8α+ cDCs and pDCs, these data suggest that CT and other Gs-protein agonists can affect IL-12 production and DC differentiation via a common mechanism involving IRF8.

CORRESPONDENCE
Brian Kelsall:
kelsall@nih.gov

Abbreviations used: cDC, conventional DC; CT, cholera toxin; CTA, CT A subunit; CTB, CT B subunit; FLT-3L, fms-related tyrosine kinase ligand; FRAP, fluorescence recovery after photobleaching; IRF, IFN regulatory factor; ISRE, IFN-stimulated response element; pDC, plasmacytoid DC; TLR, Toll-like receptor.

Cholera toxin (CT) is composed of a monomeric A subunit (CTA) and a pentameric B subunit (CTB). After binding of CTB to cell surface gangliosides, CTA acts to catalyze the ADP ribosylation of the intracellular G protein subunit Gsα, which then dissociates from Gsβγ-dimer and activates adenylate cyclase. This results in the induction of cAMP and activation of cAMP-dependent protein kinase A. Enzymatically active CT, as well as other ligands that induce cAMP production, can inhibit the production of IL-12 from monocytes and DCs (1, 2). CT also inhibits expression of IL-12β1 and -12β2 receptors on activated T cells, suppresses the function of Th1 but not Th2 T cell clones (3), and drives the differentiation of Th2 and IL-10–producing Tr1 T cells in vitro (4). In vivo, CT inhibits the production of both IL-12 and IFN-γ in mice given LPS systemically (5). Given orally with most soluble protein antigens, CT preferentially drives Th2 responses locally and systemically, which is associated with production of IgA and IgG1>IgG2a antibodies; and after repeated oral dosing, CT induces high IgE levels to coadministered antigens that results in anaphylaxis to

A. la Sala and J. He contributed equally to this paper.

The Rockefeller University Press $30.00
J. Exp. Med. Vol. 206 No. 6 1227-1235
www.jem.org/cgi/doi/10.1084/jem.20080912

subsequent antigenic challenge (6). Together with several additional effects on immune and nonimmune cells, the ability of CT to block IL-12 production and responsiveness likely contributes to its ability to drive Th2 responses when given orally with protein antigens (1).

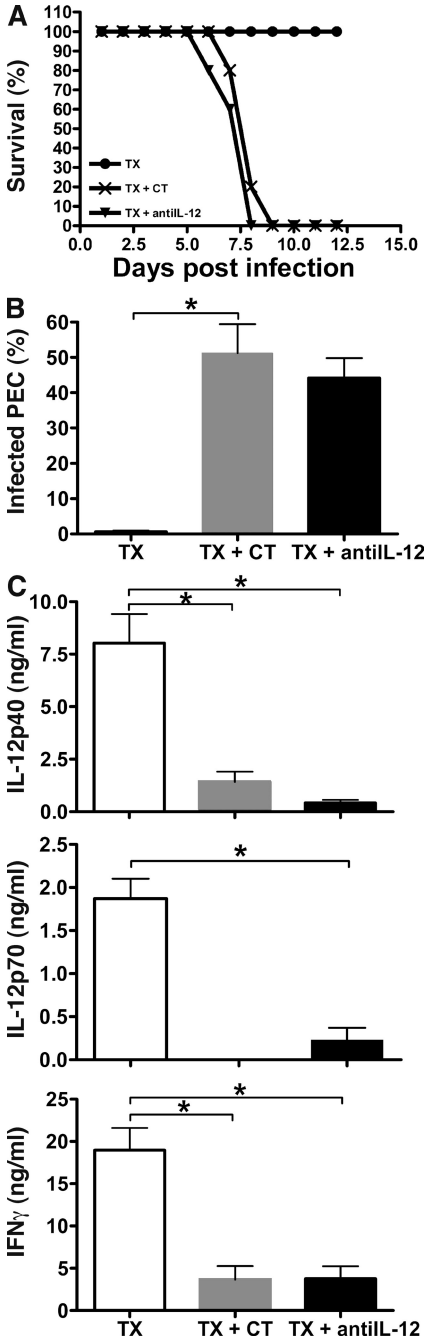

Figure 1. Reduced IL-12 and IFN-γ production in CT-treated mice results in increased parasite burden and mortality after *T. gondii* infection. (A) Survival rate of BALB/c mice infected with *T. gondii*. Mortality was monitored daily. Data shown were obtained from eight mice/group and are representative of three experiments producing similar results. (B) Parasite burden in the peritoneum was measured 5 d after infection. Results are presented as mean ± SD of five mice/group and are representative of three independent experiments. (C) Serum cytokine production after *T. gondii* infection. Sera were harvested 5 d after infection. Data shown are given as mean ± SD of 5 individual mice and are representative of three experiments that produced similar results. *, $P \leq 0.002$.

Although it has been reported that CTB alone can downregulate IL-12 expression (7), its inhibitory potency is a fraction of that caused by CT holotoxin (5). This indicates that the ability of CT to suppress IL-12 production is primarily dependent on the enzymatically active A subunit, as is its ability to act as an adjuvant in vivo (1, 2). In addition, the suppression of IL-12 by ligand-mediated activation of Gs protein–coupled receptors, such as those for prostaglandin E_2, histamine, β2-adrenergic agonists, adenosine, cannabinoids, and opiates, as well as by the cell-permeable cAMP analogue dbcAMP, suggests that the direct induction of cAMP by Gs protein activation plays a key role in CT-mediated IL-12 suppression (1, 2). However, the downstream effects of Gs protein–induced cAMP on the signaling pathways required for IL-12 production are not clear.

RESULTS AND DISCUSSION

Gs protein–mediated inhibition of IL-12 production by cDCs

Prior studies demonstrated the ability of CT to inhibit the production of IL-12 from human monocytes and monocyte-derived DCs (5). We initially determined whether this also applied to freshly isolated mouse conventional DCs (cDCs), and whether it extended to other Gs protein agonists. CT, as well as agonists for β2-adrenergic receptor (salbutamol), and the adenosine A2a receptor (CGS 21680; 2-p-[2-Carboxyethyl] phenethylamino-5-*N*-ethylcarboxamidoadenosine hydrochloride) suppressed the production of both IL-12p40 and IL-12p70 from spleen cDCs stimulated with SAC and IFN-γ (Fig. S1), whereas IL-10 production was not suppressed (unpublished data).

CT inhibits the production of IL-12 after infection with *Toxoplasma gondii* in vivo

CT has been shown to induce Th2 responses after oral administration with soluble protein antigens; however, because CT is normally given with inactivated proteins, the extent to which CT can modify the helper T (Th) cell phenotype during the induction of strong Th1 responses, as occurs after infection with intracellular pathogens, is not clear. Furthermore, when given intranasally, or orally with less purified antigens, CT has been reported to induce Th1 and Th2 responses (8, 9). Therefore, we decided to test the ability of CT to modify Th1 responses in mice during systemic infection of BALB/c mice with a high dose of the ME-49 strain of *T. gondii*. In this model, mice develop IL-12–dependent Th1 responses that clear the infection with 100% survival (10). As shown in Fig. 1, systemic administration of CT during the course of infection resulted in 100% mortality with nearly identical kinetics to that occurring after systemic neutralization of IL-12 (Fig. 1 A). In addition, parasite loads were high (Fig. 1 B) and serum levels of IL-12 and IFN-γ were suppressed in both CT and anti–IL-12–treated groups (Fig. 1 C), consistent with CT having a dominant inhibitory effect on IL-12 production and the induction of Th1 responses to this infection.

CT treatment results in a loss of CD8α⁺ cDCs

Although it is likely that a variety of cells produce IL-12 during infection with *T. gondii* in vivo, including macrophages (11) and neutrophils (12), CD8α⁺ cDCs are thought to be one major source of this essential cytokine (13). We therefore asked whether CT administration affects IL-12 production by cDC subsets in vivo. Although mice treated with CT showed a 20–30% reduction of total cell numbers in the spleen, there was a dramatic preferential reduction of CD11c⁺ CD8α⁺ cDCs compared with CD11b⁺ cDCs (Fig. 2 A) and other lymphocyte compartments (Fig. 2 B). The loss of CD8α⁺ cDCs was not caused by apoptosis (Fig. S2); was transient, with cell numbers returning to normal levels by day 6; and was dose dependent, with 5 μg of CT having maximal

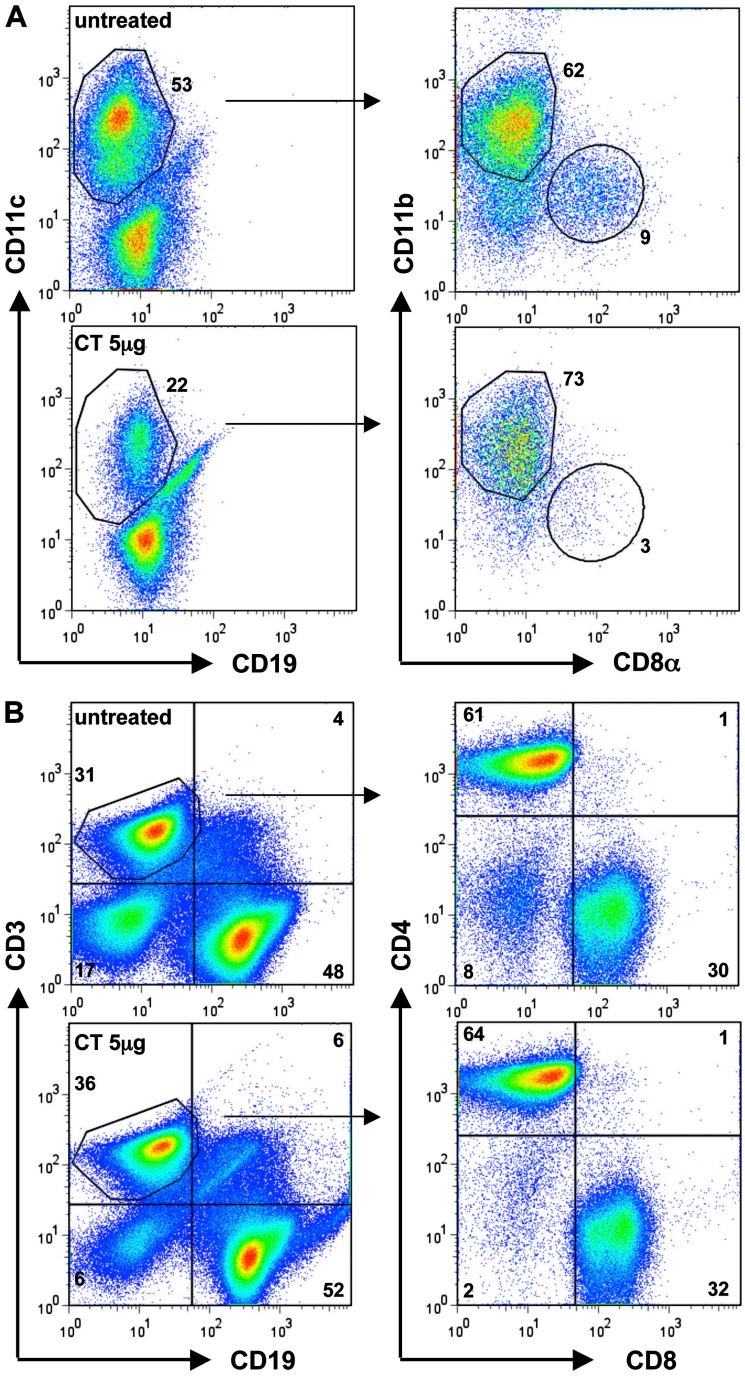

Figure 2. CT administration induces preferential loss of splenic CD8α⁺ cDCs without affecting other lymphocyte compartments in vivo. Spleen cells were isolated from BALB/c mice 48 h after i.p. CT injection and analyzed by flow cytometry. (A) MACS-enriched CD11c⁺ spleen cells. CD8α⁺ cDCs were defined as CD11c⁺CD19⁻CD8α⁺. (B) Effect of CT on T cell (CD4⁺ and CD8⁺) and B cell (CD19⁺) populations. Data shown are representative of five experiments showing similar effects (Fig. S2).

and 0.5 μg of CT having minimal effects (Fig. S3 B). Moreover, no difference in the viability of splenocytes or peripheral blood cells from CT-treated versus PBS-treated controls or CTB-treated mice was found (unpublished data). Treatment with CTB had no effect on CD8α$^+$ cDC numbers (unpublished data), indicating that ADP ribosylate activity of CTA was required for the loss of CD8α$^+$ cDCs.

The loss of IL-12–producing CD8α$^+$ cDCs may contribute to the effects seen with CT in *T. gondii* infection. To address this issue more directly, we infected mice after treatment with 0.5 μg of CT, which has only minor effects on CD8α$^+$ cDC numbers. At this dose, the effects of CT on the course of *T. gondii* infection were highly variable, yet in some experiments we observed a significant effect on survival and parasite load, despite only a minor change in CD8α$^+$ cDC numbers (Fig. S3 and not depicted). To test the possibility that CT may affect IL-12 production independent of CD8α$^+$ cDC loss, we gave graded doses of CT to mice, administered LPS systemically, and measured IL-12 and IFN-γ levels in the serum. Prior studies have shown that CD8α$^+$ cDCs are a significant source of IL-12 under these conditions (13), and that IFN-γ production after LPS administration can be blocked with antibodies to IL-12p40 (5). We found that low doses of CT (0.5 μg) consistently suppressed both IL-12 and IFN-γ production in response to LPS (Fig. S3). Furthermore, the total percentages of CD4$^+$ and CD8$^+$ T cells, as well as CD19$^+$ B cells, were unchanged after CT treatment (Fig. 2 B). These studies suggest that systemic administration of CT has two dose-dependent effects in vivo, one resulting in the loss of CD8α$^+$ cDCs and the other resulting in the inhibition of IL-12 production by DCs and possibly other cells.

CT blocks IFN regulatory factor (IRF) 8–chromatin interactions

In our initial studies using human monocytes stimulated with LPS alone or LPS and IFN-γ, CT had no effect on the activation of signaling molecules positively regulating IL-12 production, such as NF-κB, STAT-1, or the mitogen-activated

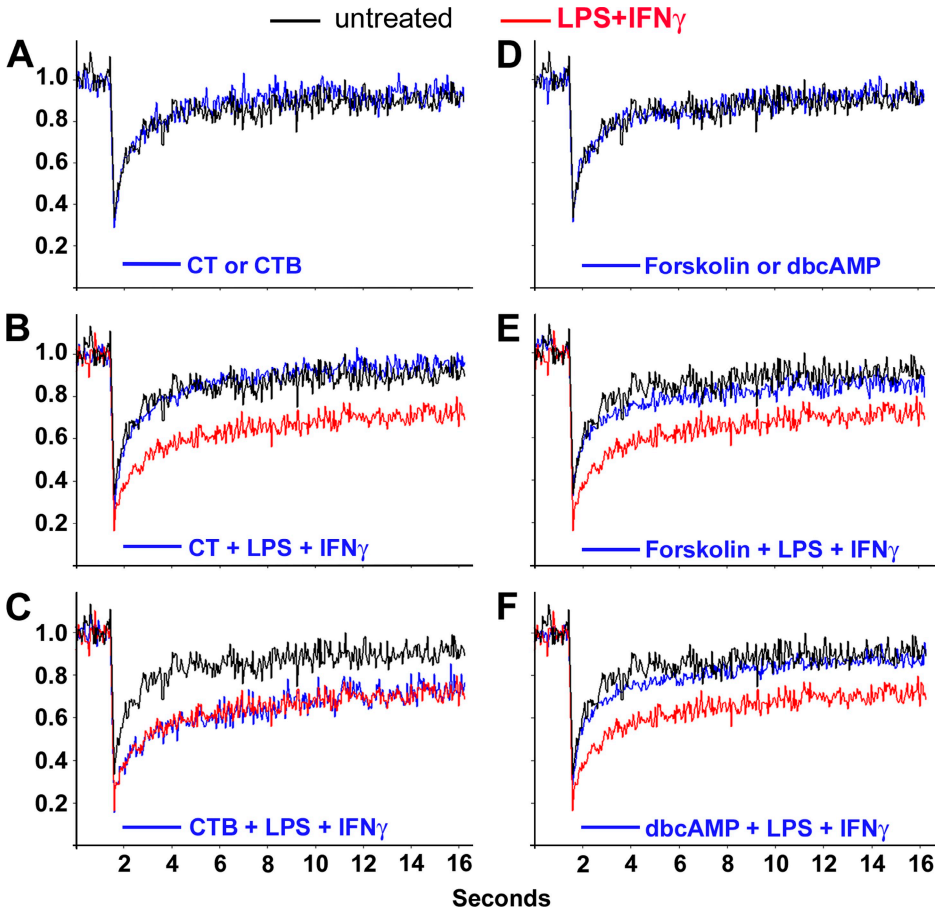

Figure 3. cAMP-elevating agents reduce IRF8–chromatin interaction elicited by LPS and IFN-γ stimulation. IRF8-deficient myeloid progenitor Tot2 cells were transduced with IRF8-GFP, left untreated (untreated), or treated with LPS (1 μg/ml) and IFN-γ (100 ng/ml) for 4 h (LPS+IFN-γ), and subjected to FRAP analysis. Where indicated, cells were exposed to CT (20 ng/ml), CTB (20 ng/ml), forskolin (20 ng/ml), or dbcAMP (100 μM) for 1 h before LPS and IFN-γ treatment. Data shown represent the mean fluorescence obtained from at least 15 independent acquisitions from a single experiment representative of three performed that yielded similar results. The response of cells treated with CT, CTB, or forskolin or dbcAMP alone is the same as that measured in untreated cells.

protein kinases (MAPKs) p38 and JNK (unpublished data). In addition, CT had no effect on the activation of extracellular signal-regulated kinase MAPK, which is a known negative regulator of IL-12 expression (unpublished data). Moreover, CT treatment did not affect the surface expression of Toll-like receptor (TLR)-4 or IFN-γ receptor on LPS-stimulated or unstimulated monocytes (unpublished data) or the IFN-γ receptor signaling pathway, as IFN-γ–induced up-regulation of HLA-DR and CD40 was unaffected (unpublished data).

We next focused our study on the effect of CT on the function of IRF8, which is a transcription factor expressed by DCs, macrophages, granulocytes, and B cells; it is a positive regulator of IL-12p35 and IL-12p40 transcription (14–17) and has a central role in the differentiation of $CD8\alpha^+$ cDC and plasmacytoid DC (pDC) populations. Furthermore, production of IL-12 in *T. gondii* infection is dependent on IRF8 (11). $IRF8^{-/-}$ mice lack the $CD8\alpha^+$ and pDCs, although they have $CD11c^+CD8\alpha^-$ cDCs (18–21). Moreover, in these mice, the residual $IRF8^{-/-}$ cDCs display impaired responsiveness to TLR-mediated signals and fail to produce IL-12p40 (18). Thus, IRF8 is essential for both IL-12 production by myeloid cells including cDCs and the development of $CD8\alpha^+$ cDCs that likely represent an IL-12–producing DC subsets during *T. gondii* infection.

We initially studied the dynamic interaction of IRF8 with chromatin in live cells using fluorescence recovery after photobleaching (FRAP) analysis, a method that was recently applied to the study of IRF8–chromatin interactions (22). For these studies, $IRF8^{-/-}$ Tot2 cells were stably transduced with IRF8-GFP that localizes to the nucleus. In the nucleus, IRF8-GFP is present in two functionally distinct forms: a fraction of low-mobility IRF8 molecules engaged in interactions with chromatin and a pool of highly mobile, unbound IRF8. As depicted in Fig. 3, in untreated IRF8-transduced Tot2 cells, a small fraction of immobile chromatin-bound IRF8 molecules was present, and 80% of the initial fluorescence signal is recovered within 4 s after photobleaching. When cells were stimulated with LPS and IFN-γ that favored IRF8–chromatin interaction, an increase in the immobile IRF8 pool, and a consequent reduction of the highly mobile unbound IRF8 fraction, occurred, resulting in significantly slower fluorescence recovery. In these samples, only 60% of the recovery occurred within the first 4 s of analysis, and the maximal recovery achieved was 70% of initial signal compared with 90% observed in untreated cells (Fig. 3, red vs. black line). Treatment with CT, but not CTB, before stimulation with LPS and IFN-γ produced a recovery curve similar to that of unstimulated cells (Fig. 3, B and C). Similar to what we observed with CT, cells pretreated with the G protein–independent adenylate cyclase activator forskolin or the membrane-permeable cAMP analogue dbcAMP and stimulated with LPS and IFN-γ displayed a quick recovery of fluorescence (Fig. 3, E and F). Importantly, treatment with CT, CTB, forskolin, or dbcAMP alone did not alter the kinetics of fluorescence recovery (Fig. 3, A and D). IRF8-GFP was not overexpressed in $IRF8^{-/-}$ Tot2 cells because levels were

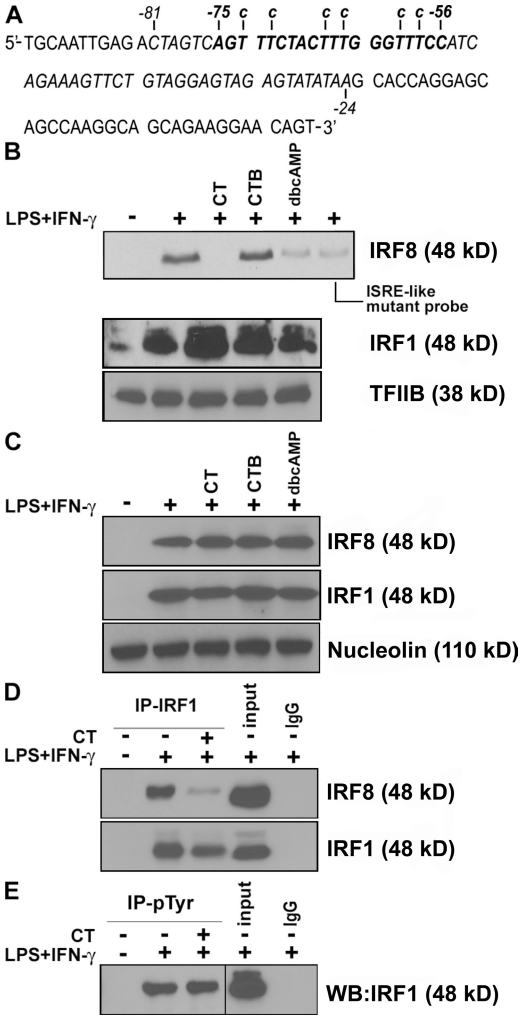

Figure 4. CT and dbcAMP reduce IRF8 binding to the ISRE-like region of the mouse IL-12p40 promoter and prevent IRF1–IRF8 heterocomplex formation. (A) Schematic representation of the −92 to +12 region of the mouse IL-12p40 promoter. The ISRE-like sequence is represented in bold. (B) CT and dbcAMP, but not CTB, inhibited IRF8, but not IRF1 or TFIIB, interaction with the mouse IL-12p40 promoter. A biotinylated DNA probe corresponding to the −81 to −24 region of the mouse IL-12p40 promoter encompassing the ISRE-like sequence, and a biotinylated mutant probe containing substitution (indicated by the lower case letters) in the context of the ISRE-like element were conjugated with streptavidin-bound magnetic beads and incubated with 500 µg of nuclear extracts from RAW 264.7 cells stimulated for 4 h as indicated. CT, CTB (both at 20 ng/ml), and dbcAMP (100 µM) were added 1 h before addition of LPS (1 µg/ml) and IFN-γ (100 ng/ml). Bound material was eluted, separated by 10% SDS-PAGE, and detected by Western blot analysis using rabbit anti-IRF8 antibody. (C) CT or dbcAMP did not modify the total amount of IRF8 or IRF1 in the nucleus. 500 µg of nuclear extracts were analyzed to measure the presence of IRF8 or IRF1 by SDS-PAGE Western blot. Membranes were stripped and reblotted to verify equal protein loading using an antinucleolin antibody. (D) CT reduces IRF1–IRF8 heterocomplex formation induced by LPS and IFN-γ. 1 mg of nuclear extract was immunoprecipitated with anti-IRF1 antibody and analyzed by Western blot for the presence of IRF8 or IRF1. (E) Tyrosine phosphorylation of IRF1 is not affected by CT. 1 mg of nuclear extracts was immunoprecipitated with antiphosphotyrosine antibody and analyzed by Western blot for the presence of IRF1. Data shown are representative of at least three experiments.

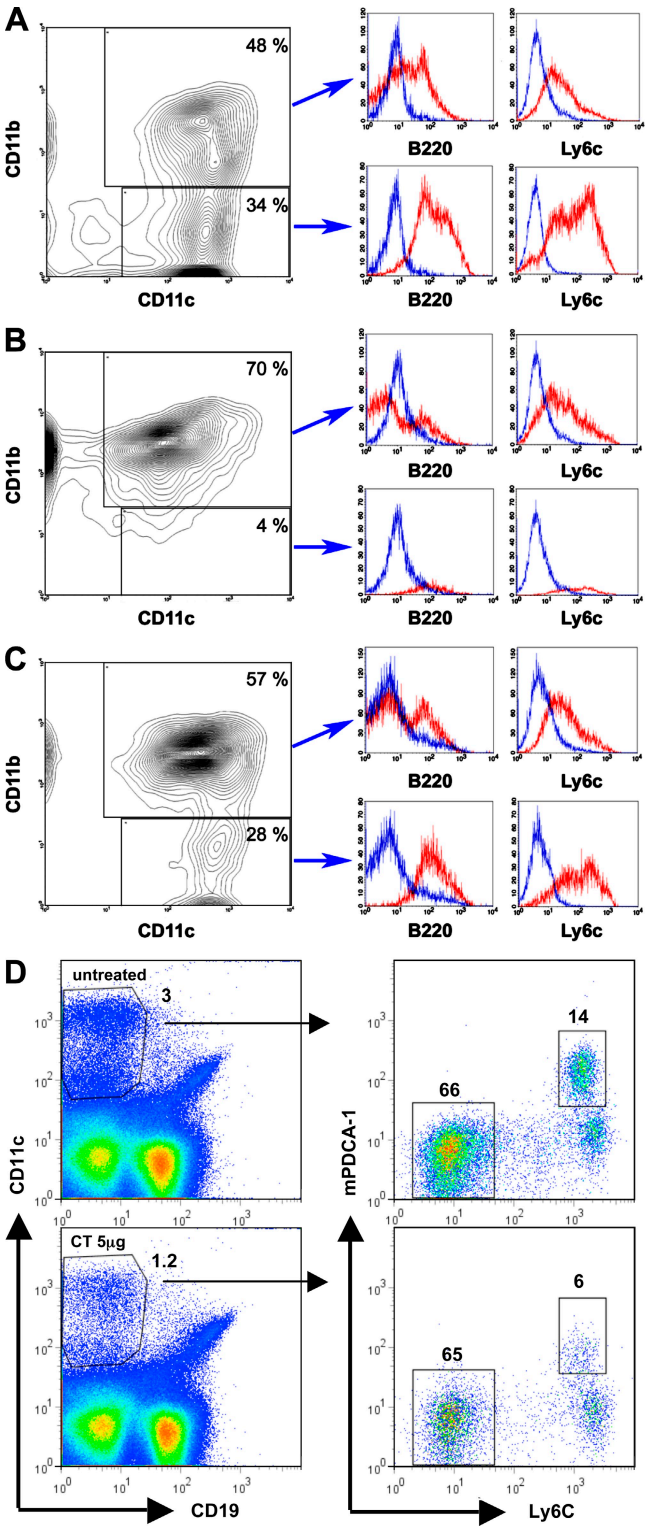

Figure 5. CT, but not CTB, blocks pDC differentiation in vitro and in vivo. (A–C) Bone marrow from BALB/c mice femurs was cultured in the presence of 100 ng/ml rh-FLT-3L with or without CT or CTB (both at 20 ng/ml). Medium was changed at day 3 and 6 of culture and fresh FLT-3L and CT or CTB was added. After 9 d, cells were harvested and subjected to flow cytometry to determine their phenotype. pDCs were defined as $CD11c^+CD11b^-B220^+Ly6C^+$. (A) Untreated. (B) CT treated. (C) CTB treated. (D) Total spleen cells from mice injected with 5 μg of CT i.p. were harvested 48 h later. pDCs are identified as $CD11c^+CD19^-mPDCA\text{-}1^+Ly6C^+$ cells. Data shown is representative of four experiments yielding similar results.

below those of endogenous IRF8 in a macrophage cell line (22). Collectively, these data indicate that increased levels of cAMP, secondary to CT-induced Gs protein ADP ribosylation, impair the ability of IRF8 to bind to chromatin, and therefore to interact with its target promoters. Interestingly, IRF8 amplifies the transcription of its own gene (23). Thus, the cAMP-dependent inhibition of IRF8 binding to its own promotor would lead to reduced IRF8 mRNA expression, a concept that is consistent with prior studies showing cAMP-dependent IRF8 mRNA down-regulation (24, 25).

CT inhibits IRF8 binding to the IL-12p40 promoter and its interaction with IRF1

IRF8 together with IRF1 has been reported to enhance IL-12p40 gene transcription induced by LPS and IFN-γ by forming a heterocomplex that interacts with a cis-acting element resembling the ISRE (IFN-stimulated response element; ISRE-like) located in the IL-12p40 mouse promoter (15, 26). To assess if CT inhibits DNA–IRF8 interaction specifically at the level of the IL-12p40 promoter, we performed a DNA affinity binding assay using a biotinylated IL-12p40 promoter sequence containing the native ISRE-like element conjugated to streptavidin beads (Fig. 4 A). As shown in Fig. 4 B, IRF8 in nuclear extracts from RAW 264.7 cells stimulated with LPS and IFN-γ bound to the probe-conjugated beads, and this binding was completely abrogated when cells were pretreated with CT, but not CTB. Moreover, a similar inhibitory effect was exerted by dbcAMP. Significantly reduced binding of IRF8 to a probe carrying a mutation in the ISRE-like element was observed (Fig. 4 B, lane 6) indicating that IRF8 binding was dependent on the integrity of the ISRE-like element.

The same ISRE-like element is a consensus sequence for IRF1 (26), therefore we investigated the effect of CT or dbcAMP on the ability of IRF1 to interact with the IL-12p40 promoter. Similar to IRF8, stimulation with LPS and IFN-γ induced IRF1 binding; however, neither CT nor dbcAMP reduced such interaction. Moreover, binding of TFIIB, a component of the RNA polymerase II complex, to the TATA box element included in the probe sequence, was unaffected by CT treatment, indicating that the inhibition exerted by CT and dbcAMP was specific for IRF8. Moreover, similar levels of IRF8 and IRF1 were detected in nuclear extracts of all cells stimulated with LPS and IFN-γ, indicating that observed effects were not caused by reduced IRF8 expression in the nucleus (Fig. 4 C).

The concomitant ability of IRF1 and inability of IRF8 to bind to the IL-12p40 promoter in cells treated with CT or dbcAMP prompted us to determine whether CT treatment

could inhibit the formation of the IRF1–IRF8 heterocomplex. Consistent with this possibility, CT markedly reduced the amount of nuclear IRF1–IRF8 complex induced by LPS and IFN-γ (Fig. 4 D). Tyrosine phosphorylation of IRF1 is a crucial event for IRF1–IRF8 complex formation (27). However, the amount of phosphorylated IRF1 induced by LPS and IFN-γ was not modified by CT (Fig. 4 E). This indicates that the ability of CT to block IRF1–IRF8 complex formation is not caused by impaired IRF1 phosphorylation.

Together with IL-12 suppression, CT can enhance the ability of TLR ligands to induce DC production of IL-6, IL-1β, and IL-10, while inhibiting their production of TNF-α (4). We confirmed the ability of CT and dbcAMP to inhibit the production of IL-12 and TNF-α, but not IL-10, in human peripheral blood monocytes, monocyte-derived DCs, and the RAW 264.7 cell line stimulated with LPS and IFN-γ (Fig. S4). Interestingly, recent data indicate that TNF-α gene transcription in mouse macrophages is also regulated by IRF1 and IRF8 (28). Therefore, it is feasible that the mechanism by which CT and cyclic AMP blocks TNF-α production is also caused by effects on IRF1–IRF8 interactions. The molecular events triggered by CT that lead to reduced IRF1–IRF8 interaction remain unclear. In addition to IRF1, IRF8 has been reported to form heterocomplexes with other binding partners, including NFAT and PU.1. Interference with physical interaction between these proteins and IRF8 might regulate its ability to associate with DNA and IRF1. In support of this possibility, increased cAMP levels have been reported to inhibit NFAT activity (29). PKA-dependent phosphorylation of NFAT increased 14–3-3 binding and reduced NFAT transcription activity at the IL-2 promotor. Whether CT and other cAMP inducers might affect such interactions is currently under investigation in our laboratories.

CT blocks the differentiation of pDCs from bone-marrow cells cultured with fms-related tyrosine kinase 3 ligand (FLT-3L) in vitro and mouse spleen cells in vivo

Results of the FRAP analysis indicate that CT induces a general inhibition of IRF8 function, suggesting that other IRF8-dependent processes might also be affected. IRF8 plays a key role not only in the activation of IL-12p35 and p40 genes, but also in the normal development of pDC and $CD8\alpha^+$ cDC populations in vivo (18–21). Moreover, IRF8-deficent bone marrow cells fail to differentiate into pDCs when cultured in the presence of FLT-3L in vitro (21). We therefore studied the effect of CT on the generation of pDCs from FLT-3L–stimulated bone marrow cultures. In keeping with previous reports, after culture with FLT-3L, one third of mouse bone marrow cells differentiated into $CD11c^+$ $CD11b^-$ cells that also expressed B220 and Ly6c and could therefore be identified as pDCs (Fig. 5 A). In the presence of CT, we observed a dramatic reduction of the $CD11c^+CD11b^-$ subset (from 34.6 to 4.28%), and a concomitant increase in the $CD11c^+CD11b^+$ population. In addition, only 50% of the remaining $CD11c^+CD11b^-$ cells expressed Ly6C (Fig. 5 B). Conversely, exposure to CTB did not alter FLT-3L–induced pDC differentiation (Fig. 5 C), indicating that this effect of CT is dependent on the CTA activity. Consistent with these results, and similar to our findings with $CD8\alpha^+$ DCs, pDCs were preferentially lost after CT treatment in vivo (Fig. 5 D). The ability of CT to inhibit the differentiation of pDCs from FLT-3L–treated bone marrow and to induce pDC depletion in vivo is consistent with the hypothesis that IRF8–DNA interaction is a major target of CT activity.

In summary, our findings indicate that CT can inhibit IL-12 production in vivo after infection with *T. gondii*, or systemic administration of LPS. In addition, we identify the inhibition of IRF8 function as a major molecular mechanism by which CT and other cAMP-inducing agents prevent IL-12 production in vitro and in vivo. Furthermore, we demonstrate that the CT-induced block of IRF8 function is associated with impaired IRF1–IRF8 heterocomplex formation that is independent of the phosphorylation state of IRF1. Finally, by blocking IRF8 function, CT may simultaneously inhibit IL-12p40 mRNA expression in macrophages and differentiated DCs and interfere with normal differentiation of $CD8\alpha^+$ DCs (and pDCs) that represent a primary source of IL-12, at least under certain stimulation conditions.

MATERIALS AND METHODS

Mice and cell lines. 8–12-wk-old conventionally housed female BALB/c mice were obtained from the National Cancer Institute and were used as approved under animal study protocol LMI11E by the National Institute of Allergy and Infectious Disease/National Institutes of Health (NIH) Animal Care and Use Committee. The derivation and maintenance of $IRF8^{-/-}$ Tot2 cells and their transfection with IRF8-GFP were previously described (30). The mouse macrophage cell line RAW 264.7 was purchased from American Type Culture Collection (ATCC).

Cell culture and measurement of cytokines. $CD11c^+$ splenocytes were isolated using anti–mouse-CD11c immunomagnetic beads (Miltenyi Biotech). Human monocytes were obtained by counterflow centrifugation-elutriation of blood collected from normal blood donors under the NIH Institutional Review Board–approved human subjects protocol 99-cc-0168. Monocyte-derived DCs were obtained by culturing purified human monocytes in GMCSF and IL-4, as previously described (5). The mouse macrophage cell line RAW 264.7 was and stimulated at 80% confluence. $CD11c^+$ splenocytes, human blood monocytes, monocyte-derived DCs (Mo-DC), or the RAW 264.7 cells were cultured at 1–2 × 10^6 cells/ml in RPMI-1640 and supplemented with 10% FCS, 100 μg/ml penicillin, 100 μg/ml streptomycin, 50 μg/ml gentamicin, 5% NCTC-109 media (all from Invitrogen), 15 mM Hepes, and 200 mM glutamine (cRPMI) at 37°C and 5% CO_2 with various stimuli as indicated. CT was purchased from List Biological Laboratories. *Staphylococcus aureus*, Cowan's strain I (SAC; Pansorbin) was obtained from Calbiochem. Recombinant mouse IFN-γ was obtained from BD. LPS (from *Escherichia coli*, serotype 0127:B8) and salbutamol were purchased from Sigma-Aldrich. Anti–mouse–IL-12 (clone C17.6) was originally provided by G. Trinchieri (National Cancer Institute, Bethesda, MD). CGS21680 and ZM241385 were obtained from Tocris Bioscience. Cytokine levels in cell culture supernatants and mouse sera were measured by ELISA using standard kits (BD). ELISA lower limit of detection was 50 pg/ml for IFN-γ and IL-12 p70 and 30 pg/ml for IL-12 p40.

***T. gondii* infection.** *T. gondii* cysts (ME-49 strain) were prepared from brains of infected mice as previously described (31). BALB/c mice were untreated or treated with two doses of CT (5 μg) or anti–IL-12 antibody (1.8 mg) given

i.p. at 3-d intervals. Mice were infected with 100 cysts given i.p. 1 d after the first dose of CT or anti–IL-12. The percentage of infected peritoneal exudate cells was determined using stained cytospin preparations. 500 cells were counted for each sample. 5 d after infection with *T. gondii*, blood was collected from individual mice for cytokine quantification.

FACS analysis. Spleen cells, or $CD11c^+$ enriched splenocytes were analyzed by flow cytometry using antibodies for cDCs (anti-CD11c, HL3), B cells (anti-CD19, 1D3), T cells (anti-CD3, 145-2C11, anti-CD4, GK1.5, anti-CD8, Ly-2), and pDCs (anti-B220, RA3-6B2, anti-Ly-6C, AL-21, mPDCA-1, JF05-1C2.4.1; all from BD). Labeled cells were analyzed using a FACSCalibur flow cytometer (BD), and data was analyzed using FlowJo software (Tree Star, Inc.).

FRAP. FRAP for IRF8-chromatin interactions was performed on IRF8-GFP–transduced $IRF8^{-/-}$ Tot2 cells as previously described (22). Tot2 cells plated on a chambered coverslip in 1% methylcellulose (MethoCult; Stem Cell Technologies) were kept at 37°C by using an air stream stage incubator (ASI 400; Nevtek). Live-cell imaging was performed on a 510 confocal microscope (Carl Zeiss, Inc.) by using the 488-nm line of an Ar laser with a 100×, 1.3-numerical aperture oil immersion objective. Photobleaching was performed on a small circular area (0.5-μm radius, 25 pixels) in the nucleus at the maximum laser power. 30 prebleach images were acquired before a bleach pulse of 115 ms. Fluorescence recovery was monitored at low laser intensity (0.2% of a 45-mW laser) at 45-ms intervals for 16 s. FRAP experiments were performed on at least 15 independent cells, and data were averaged to generate a single FRAP curve. FRAP data obtained using cells before and after stimulation with LPS+IFN-γ were analyzed to fit to the recently developed mathematical binding models to confirm and support our initial hypothesis on the two fractions of IRF8 (32).

DNA affinity binding assay and immunoprecipitation. Nuclear extracts from RAW 264.7 cells were obtained using NE-PER extraction kit following manufacturer's instructions. 5′-Biotin-labeled DNA sequence corresponding to the −81 to −24 region of the murine IL-12p40 promoter containing a known ISRE-like element, as well as a control sequence containing a substitution mutation in the region of the ISRE-like element were purchased from Invitrogen. Biotin-labeled probes were conjugated to 200 μg of streptavidin-coated magnetic beads (Dynabeads M-280 streptavidin; Dynal) in Tris-EDTA buffer (pH 7.9) and were blocked with 0.5% bovine serum albumin in TGED buffer (10 mM Tris–HCl, pH 8.0, 10% vol/vol glycerol, 0.1 mM ethylenediaminetetraacetic acid, and 0.01% Triton X-100) overnight at 4°C. The mixtures of probe-conjugated beads and 500 μg of nuclear extracts in 500 μl of TGED with the final concentration of NaCl at 100 mM were subsequently incubated at 4°C for 4 h. Beads were extensively washed with TGED buffer, and DNA-bound proteins were eluted using TGED with 1 M NaCl. Proteins were separated by SDS-PAGE for immunoblot detection with rabbit anti-IRF8 antibody. For coimmunoprecipitations, 500 μg of nuclear extracts from RAW264.7 cells diluted 1:3 with wash buffer (50 mM Tris-HCl, 1 mM PMSF, Complete protease inhibitor cocktail [Roche], and phosphatase inhibitor cocktail 1 and 2 [Sigma-Aldrich]) were incubated with mouse monoclonal anti-IRF1 (2.5 μg/sample; Santa Cruz Biotechnology, Inc.) or irrelevant IgG over night at 4°C in a rotator and recovered with 25 μl of G protein–conjugated magnetic beads (Active Motifs). Samples were subjected to SDS-PAGE and Western blot analysis with rabbit anti-IRF8 or rabbit anti-IRF1 (Santa Cruz Biotechnology). For determining IRF1 phosphorylation, mouse anti-phosphotyrosine monoclonal cocktail (5 μl/sample, 4G10; Millipore) or 2.5 μg of irrelevant IgG were incubated overnight at 4°C with 25 μl G protein–conjugated magnetic beads. Beads were then washed twice with ice-cold PBS and incubated (90 min at 4°C in a rotator) with 1 mg of nuclear extract. After extensive washing, samples were subjected to SDS-PAGE and Western blot analysis with rabbit anti-IRF1 antibody (Santa Cruz Biotechnology, Inc.).

Bone marrow–derived pDCs. Bone marrow from 6-wk-old mice was cultured at 5×10^5 cells/ml in D-MEM (Biofluids, Inc.) supplemented with 10% fetal bovine serum and containing 100 ng/ml recombinant human FLT-3L (PeproTech). Medium together with FLT-3L was changed at days 3 and 6 of culture. CT or CTB was added at 20 ng/ml final concentration at the beginning of the culture and at every medium change. After 9 d, cells were analyzed by flow cytometry using fluorochrome-conjugated monoclonal antibodies against CD11c, CD11b, B220, and Ly6C (BD).

Statistical analysis. Results represent the mean ± SD where applicable. Statistical significance of differences was determined by the Student's *t* test.

Online supplemental material. Fig. S1 demonstrates the regulation of IL-12 production from murine cDCs by the β_2 adrenergic agonist Salbutamol, the adenosine A2a receptor agonist CGS21680, the adenosine A2a receptor antagonist ZM241385 and CT. Fig. S2 shows the time course of $CD8\alpha^+$ cDC loss as well as annexin V staining of $CD8\alpha^+$ cDCs after CT administration in vivo. Fig. S3 demonstrates the effect of CT dose on $CD8\alpha^+$ DC loss, and the effect on IL-12 and IFN-γ production in vivo. Fig. S4 demonstrates the effect of CT and dbcAMP on IL-12, TNF-α, and IL-10 production from human monocytes, monocyte-derived DCs, and RAW 264.7 cells. Online supplemental material is available at http://www.jem.org/cgi/content/full/jem.20080192/DC1.

This work was supported by research funds from the Division of Intramural Research, National Institutes of Allergy and Infectious Diseases, National Institutes of Health.
The authors have no conflicting financial interests.

Submitted: 25 April 2008
Accepted: 4 May 2009

REFERENCES

1. Braun, M.C., and B.L. Kelsall. 2001. Regulation of interleukin-12 production by G-protein-coupled receptors. *Microbes Infect.* 3:99–107.
2. Vandenbroeck, K., I. Alloza, M. Gadina, and P. Matthys. 2004. Inhibiting cytokines of the interleukin-12 family: recent advances and novel challenges. *J. Pharm. Pharmacol.* 56:145–160.
3. Munoz, E., A.M. Zubiaga, M. Merrow, N.P. Sauter, and B.T. Huber. 1990. Cholera toxin discriminates between T helper 1 and 2 cell receptor-mediated activation: role of cAMP in T cell proliferation. *J. Exp. Med.* 172:95–103.
4. Lavelle, E.C., A. Jarnicki, E. McNeela, M.E. Armstrong, S.C. Higgins, O. Leavy, and K.H.G. Mills. 2004. Effects of cholera toxin on innate and adaptive immunity and its application as an immunomodulatory agent. *J. Leukoc. Biol.* 75:756–763.
5. Braun, M.C., J. He, C.-Y. Wu, and B.L. Kelsall. 1999. Cholera toxin suppresses interleukin (IL)-12 production and IL-12 receptor beta 1 and beta 2 chain expression. *J. Exp. Med.* 189:541–552.
6. Li, X.M., B.H. Schofield, C.K. Huang, G.I. Kleiner, and H.A. Sampson. 1999. A murine model of IgE-mediated cow's milk hypersensitivity. *J. Allergy Clin. Immunol.* 103:206–214.
7. Boirivant, M., I.J. Fuss, L. Ferroni, M. De Pascale, and W. Strober. 2001. Oral administration of recombinant cholera toxin subunit B inhibits IL-12-mediated murine experimental (trinitrobenzene sulfonic acid) colitis. *J. Immunol.* 166:3522–3532.
8. Bourguin, I., T. Chardes, and D. Bout. 1993. Oral immunization with *Toxoplasma gondii* antigens in association with cholera toxin induces enhanced protective and cell-mediated immunity in C57BL/6 mice. *Infect. Immun.* 61:2082–2088.
9. Debard, N., D. Buzoni-Gatel, and D. Bout. 1996. Intranasal immunization with SAG1 protein of *Toxoplasma gondii* in association with cholera toxin dramatically reduces development of cerebral cysts after oral infection. *Infect. Immun.* 64:2158–2166.
10. Gaddi, P.J., and G.S. Yap. 2007. Cytokine regulation of immunopathology in toxoplasmosis. *Immunol. Cell Biol.* 85:155–159.

11. Scharton-Kersten, T., C. Contursi, A. Masumi, A. Sher, and K. Ozato. 1997. Interferon consensus sequence binding protein-deficient mice display impaired resistance to intracellular infection due to a primary defect in interleukin 12 p40 induction. *J. Exp. Med.* 186:1523–1534.
12. Bliss, S.K., B.A. Butcher, and E.Y. Denkers. 2000. Rapid recruitment of neutrophils containing prestored IL-12 during microbial infection. *J. Immunol.* 165:4515–4521.
13. Reis e Sousa, C., S. Hieny, T. Scharton-Kersten, D. Jankovic, H. Charest, R.N. Germain, and A. Sher. 1997. In vivo microbial stimulation induces rapid CD40 ligand-independent production of interleukin 12 by dendritic cells and their redistribution to T cell areas. *J. Exp. Med.* 186:1819–1829.
14. Wang, I.-M., C. Contursi, A. Masumi, X. Ma, G. Trinchieri, and K. Ozato. 2000. An IFN-{gamma}-inducible transcription factor, IFN consensus sequence binding protein (ICSBP), stimulates IL-12 p40 expression in macrophages. *J. Immunol.* 165:271–279.
15. Masumi, A., S. Tamaoki, I.-M. Wang, K. Ozato, and K. Komuro. 2002. IRF-8/ICSBP and IRF-1 cooperatively stimulate mouse IL-12 promoter activity in macrophages. *FEBS Lett.* 531:348–353.
16. Zhu, C., K. Rao, H. Xiong, K. Gagnidze, F. Li, C. Horvath, and S. Plevy. 2003. Activation of the murine interleukin-12 p40 promoter by functional interactions between NFAT and ICSBP. *J. Biol. Chem.* 278:39372–39382.
17. Liu, J., X. Guan, T. Tamura, K. Ozato, and X. Ma. 2004. Synergistic activation of interleukin-12 p35 gene transcription by interferon regulatory factor-1 and interferon consensus sequence-binding protein. *J. Biol. Chem.* 279:55609–55617.
18. Schiavoni, G., F. Mattei, P. Sestili, P. Borghi, M. Venditti, H.C. Morse III, F. Belardelli, and L. Gabriele. 2002. ICSBP is essential for the development of mouse type I interferon-producing cells and for the generation and activation of CD8α^+ dendritic cells. *J. Exp. Med.* 196:1415–1425.
19. Aliberti, J., O. Schulz, D.J. Pennington, H. Tsujimura, C. Reis e Sousa, K. Ozato, and A. Sher. 2003. Essential role for ICSBP in the in vivo development of murine CD8alpha + dendritic cells. *Blood.* 101:305–310.
20. Tsujimura, H., T. Tamura, C. Gongora, J. Aliberti, C. Reis e Sousa, A. Sher, and K. Ozato. 2003. ICSBP/IRF-8 retrovirus transduction rescues dendritic cell development in vitro. *Blood.* 101:961–969.
21. Tsujimura, H., T. Tamura, and K. Ozato. 2003. Cutting edge: IFN consensus sequence binding protein/IFN regulatory factor 8 drives the development of type I IFN-producing plasmacytoid dendritic cells. *J. Immunol.* 170:1131–1135.
22. Laricchia-Robbio, L., T. Tamura, T. Karpova, B.L. Sprague, J.G. McNally, and K. Ozato. 2005. Partner-regulated interaction of IFN regulatory factor 8 with chromatin visualized in live macrophages. *Proc. Natl. Acad. Sci. USA.* 102:14368–14373.
23. Kantakamalakul, W., A.D. Politis, S. Marecki, T. Sullivan, K. Ozato, M.J. Fenton, and S.N. Vogel. 1999. Regulation of IFN consensus sequence binding protein expression in murine macrophages. *J. Immunol.* 162:7417–7425.
24. Hickey, F.B., C.F. Brereton, and K.H.G. Mills. 2008. Adenylate cycalse toxin of *Bordetella pertussis* inhibits TLR-induced IRF-1 and IRF-8 activation and IL-12 production and enhances IL-10 through MAPK activation in dendritic cells. *J. Leukoc. Biol.* 84:234–243.
25. Spensieri, F., G. Fedele, C. Fazio, M. Nasso, P. Stefanelli, P. Mastrantonio, and C.M. Ausiello. 2006. *Bordetella pertussis* inhibition of interleukin-12 (IL-12) p70 in human monocyte-derived dendritic cells blocks IL-12 p35 through adenylate cyclase toxin-dependent cyclic AMP induction. *Infect. Immun.* 74:2831–2838.
26. Maruyama, S., K. Sumita, H. Shen, M. Kanoh, X. Xu, M. Sato, M. Matsumoto, H. Shinomiya, and Y. Asano. 2003. Identification of IFN regulatory factor-1 binding Site in IL-12 p40 gene promoter. *J. Immunol.* 170:997–1001.
27. Sharf, R., D. Meraro, A. Azriel, A.M. Thornton, K. Ozato, E.F. Petricoin, A.C. Larner, F. Schaper, H. Hauser, and B.Z. Levi. 1997. Phosphorylation events modulate the ability of interferon consensus sequence binding protein to interact with interferon regulatory factors and to bind DNA. *J. Biol. Chem.* 272:9785–9792.
28. Vila-del Sol, V., C. Punzon, and M. Fresno. 2008. IFN-{gamma}-induced TNF-{alpha} expression is regulated by interferon regulatory factors 1 and 8 in mouse macrophages. *J. Immunol.* 181:4461–4470.
29. Chow, C.W., and R.J. Davis. 2000. Integration of calcium and cyclic AMP signaling pathways by 14-3-3. *Mol. Cell. Biol.* 20:702–712.
30. Tamura, T., T. Nagamura-Inoue, Z. Shmeltzer, T. Kuwata, and K. Ozato. 2000. ICSBP directs bipotential myeloid progenitor cells to differentiate into mature macrophages. *Immunity.* 13:155–165.
31. Gazzinelli, R., Y. Xu, S. Hieny, A. Cheever, and A. Sher. 1992. Simultaneous depletion of CD4+ and CD8+ T lymphocytes is required to reactivate chronic infection with Toxoplasma gondii. *J. Immunol.* 149:175–180.
32. Sprague, B.L., R.L. Pego, D.A. Stavreva, and J.G. McNally. 2004. Analysis of binding reactions by fluorescence recovery after photobleaching. *Biophys. J.* 86:3473–3495.